

# Rx Craft, a Manned Model of the RCN Hydrofoil Ship "Bras d'Or"

E. A. JONES\*

*Naval Research Establishment, Defense Research Board, Canada*

Rx, a versatile hydrofoil test craft, was designed and constructed to investigate the characteristics of different hydrofoil configurations and to allow rapid change of hydrofoil design parameters. Her major use has been in a prolonged series of development tests to assist the DeHavilland Aircraft Company of Canada in the design of the Royal Canadian Navy's (RCN's) 200-ton hydrofoil ship "Bras d'Or" (FHE-400). For this purpose she was equipped with a canard, surface-piercing hydrofoil system and operated as a quarter-scale dynamic model. The development period saw the introduction of superventilating sections at the FHE-400 bow foil, and the refinement and test of these comparatively little-known sections on model scale formed a large part of the work described. Performance tests in exacting rough-water conditions showed the system to operate well in a seaway, and test data and trials experience throughout the development period demonstrated convincingly the value of the large-scale manned model, with six degrees of freedom and rough-water capability, in the development of advanced marine vehicles.

## Introduction

THE Naval Research Establishment (NRE) of the Canadian Defense Research Board has been engaged in hydrofoil research since 1951. In 1959 and 1960, this research resulted in an NRE proposal for a 200-ton, 50- to 60-knot, open-ocean antisubmarine hydrofoil ship which has subsequently been designed by DeHavilland Aircraft of Canada Ltd. for the Royal Canadian Navy (RCN).<sup>1</sup> The resultant prototype ship HMCS "Bras d'Or" (FHE-400) is currently under construction at Sorel, Quebec, and is illustrated in Fig. 1.

Since 1961, NRE's major contribution to this project has been the use of its  $3\frac{1}{2}$ -ton research craft Rx, shown in Fig. 2, as a manned quarter-scale dynamic model of the FHE-400 hydrofoil system. Experiments conducted with six degrees of freedom, in rough water and turns, have provided results not obtainable by conventional hydrodynamic laboratory facilities. Although the original intention was to use Rx primarily to check DeHavilland's analog computer and design predictions for the dynamic behavior of the FHE-400 system foiborne in a seaway, events proved that Rx had a more important role to play in demonstrating problem areas which would have been overlooked by conventional design and model test techniques. Considerable test and development work was required on the hydrofoil system to achieve optimum rough-water performance, and development trials assumed prime importance.

This paper describes the design of Rx and its equipment and examines its use in developing the FHE-400 hydrofoil system.

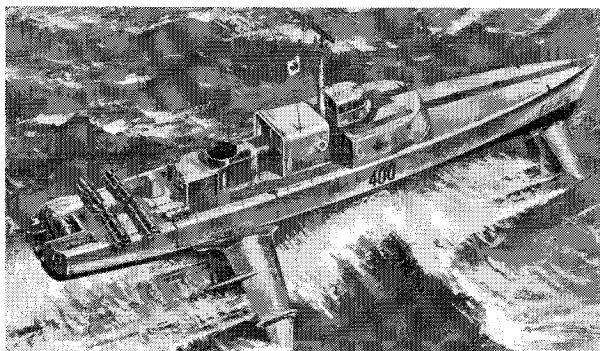


Fig. 1 HMCS "Bras d'Or" (FHE-400).

Presented as Paper 66-730 at the AIAA/USN 2nd Marine Systems and ASW Conference, Los Angeles-Long Beach, Calif., August 9-10, 1966; submitted September 9, 1966. [1.08, 6.14, 7.07, 10.11]

\* Defense Scientific Service Officer.

An important purpose of the paper is to illustrate the value of open-water tests with a manned model as an integral part of the design process for advanced marine vehicles.

## Craft Design

Inexpensive to build but thoroughly versatile, Rx was designed in 1955 as a hydrofoil research tool to allow investigation of different hydrofoil configurations and to allow quick and easy changes to such basic features as foil base length, load distribution, and foil unit geometry, as well as to the sections and incidences of the foils themselves. She is sufficiently large and fast to allow reasonable scaling and to accommodate a worthwhile instrumentation payload but small enough to allow easy handling and maintenance by a small team and keep both first costs and the cost of making changes comparatively low.

It was assumed from the start that the craft would be used for foiborne performance tests only, and the hull was designed to be as simple as reasonable strength, seaworthiness, and resistance considerations would allow. The gunwales are straight and parallel over the whole hull length and are reinforced with aluminum rails. The rails simplify the mounting of the cross beam to which the main foil units are secured and enable it to be stationed readily at any point along the hull length. For three-point configurations, great flexibility in foil base length and load distribution is provided by the use of a telescoping tube to carry the third hydrofoil unit. This tube can be fitted at the bow, as required for the FHE-400 canard configuration shown in Fig. 2, but can also be fitted at the stern. Stern mounting was employed in earlier tests on ladder hydrofoils in an orthodox configuration, and this arrangement is shown in Fig. 3.

The hull length is 25 ft, which gives the right foil base length and travel for quarter-to half-scale modelling of current hydrofoil craft designs. It also makes possible a reasonable hull

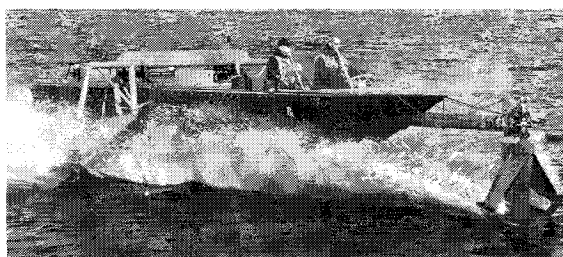


Fig. 2 Rx with FHE-400 foils.

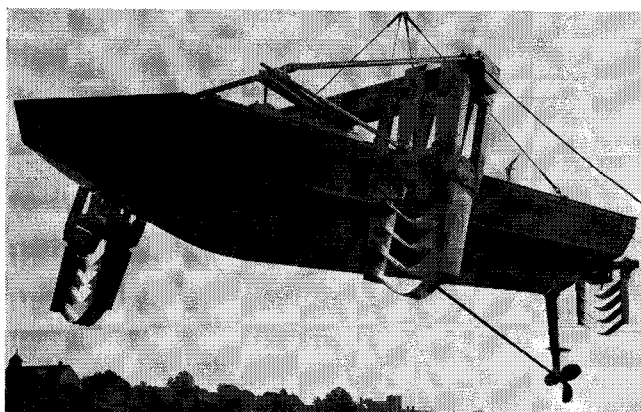


Fig. 3 Rx with ladder foils.

clearance without too great a propeller shaft inclination. The hull is completely prismatic over much of its length, with vertical top sides and a V bottom. A high deadrise of  $25^\circ$  was selected for low hull pounding when foilborne in waves, and the breadth of 6 ft was considered minimal for reasonable static stability with this deadrise. The hull depth of 3 ft was chosen to keep the foil beam close to the water and to alleviate moments at the foil mountings.

The hull structure is exceptionally strong and is based on two main longitudinal members spaced 21 in. apart. These are laminated from  $\frac{3}{8}$ -in. fir plywood to a thickness of  $1\frac{1}{2}$  in., increased to  $1\frac{7}{8}$  in. in the midships section where they serve as engine bearers. Frames are spaced on 18-in. centers and are of 1- $\times$ -2-in. fir with  $\frac{3}{8}$ -in. plywood knees and floors. All joints are screwed and glued. The hull skin is  $\frac{3}{8}$ -in. plywood and, in recent years, has had an exterior thin covering of fiberglass mat primarily to reduce water absorption and maintenance.

Water screw propulsion was chosen to allow the possibility of experimental research on propellers and pod systems. The selected power plant was a rugged, water-cooled Chrysler Imperial Type M-45 marine engine. This was fairly heavy for its normal rating of 235 hp but was preferred to a car engine because of its anticipated reliability under arduous marine working conditions. The weight penalty was offset to a great extent by modification at NRE, which increased the engine power to 365 hp at 4500 rpm through use of a Latham

supercharger, special carburetion, racing cam shafts, and strengthened connecting rods.

The location of the heavy engine was determined by center-of-gravity requirements. It is installed horizontally, and a V-drive gearbox with a 2.05:1 reduction ratio brings the shaft out at an inclination of  $20^\circ$ . A single, cast-aluminum shaft support strut is located at the stern and carries an internal duct with a scoop at the lower end to pick up cooling water. The 22-in.-diam propeller used for most tests is of conventional design with a pitch of 21 in. Fuel is carried in two 15-gal tanks located in the engine bay close to the center of gravity.

The internal layout of the craft as equipped for FHE-400 trials is shown in Fig. 4. Watertight bulkheads located forward of the engine compartment and immediately abaft the cockpit position form the end walls of buoyancy tanks filled with plastic foam. These, with the watertight instrumentation compartment aft, are sufficient to float the craft if otherwise flooded. The original intention was to leave the engine compartment open, but heavy spray affected engine performance and aluminum decking and hatches had to be provided.

### Rx as an FHE-400 System Model

The outlines of FHE-400 and Rx are compared in Fig. 5. The hull shapes are very different, but this is unimportant since foilborne performance was of prime concern. However, hull clearance on Rx is restricted to 23 in. to obtain adequate propeller immersion, and this is about 11 in. too low to model correctly the FHE-400 clearance of 11 ft 6 in. at 60 knots. This undoubtedly affects Rx performance adversely in a seaway, particularly at lower foilborne speeds.

The Rx foil system was designed and built by DeHavilland at a very early stage in the development program. It is of the same general type as that for FHE-400, and the original geometry is shown in Fig. 6 and Table 1. The bow foil, although modified many times, continually reflected full-scale design progress very closely. Because of instrumentation and structural requirements, the main foils differed from those of FHE-400 from the start, and, although some changes were made, these differences became increasingly significant as the design progressed. In Rx, the main foil struts slope outwards to clear the hull and thus allow measurement of foil loads by dynamometers in the foil beam structure. The main foil structure is complicated also by the need for structural stays

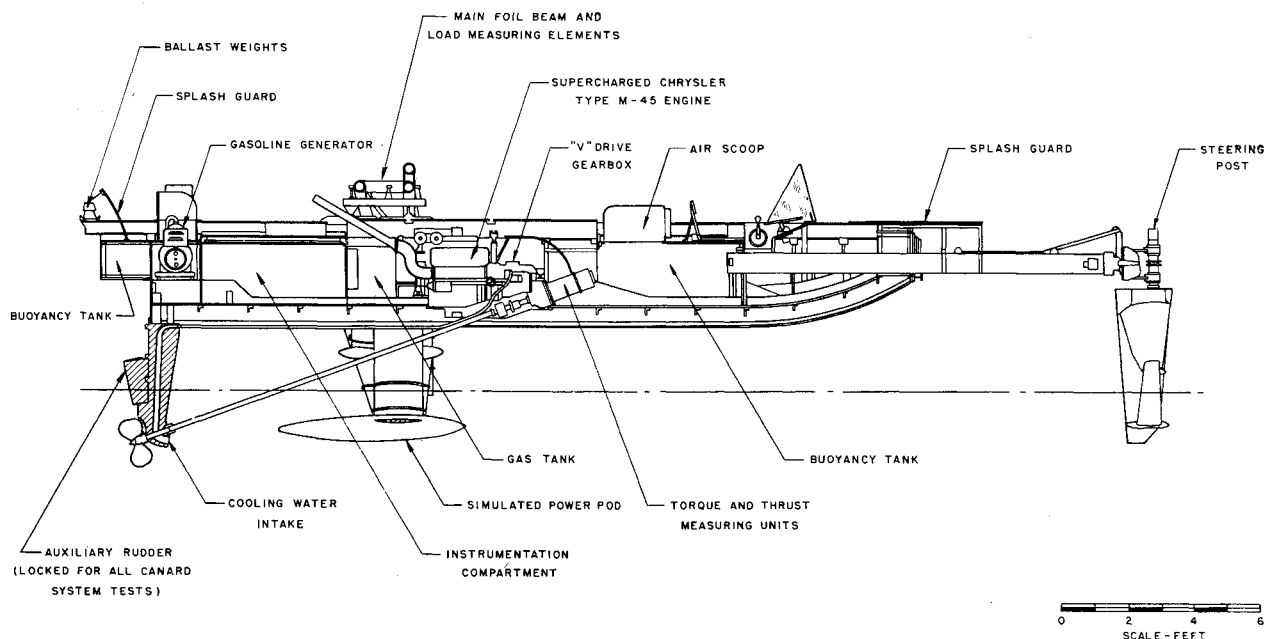


Fig. 4 Hull cross section

from the foil beam to the outer main foil intersections. In the final FHE-400 design, the anhedral extensions are canted down and made incidence-controlled to augment lateral stability at intermediate speeds; but they remained fixed extensions of the upper panels in Rx. The full-scale main foil sections were specially developed<sup>2</sup> to delay the onset of cavitation and differ greatly in chord and thickness ratio from the standard NACA and Walchner sections used in Rx.

The Rx foils were machined from solid hard-anodized 75 ST aluminum, except for the upper main anhedral panels which were fabricated from aluminum sheet. Foils and struts are pin-jointed at all intersections. The bow foil is adjustable in rake from the driver's position by means of an electric actuator, thus providing a ready means of changing bow foil incidence settings. It is also possible to change the rake of the main foil unit by adjustment screws in the mountings of the main foil beam structure.

The propulsion arrangements are very different. In FHE-400, there are two sets of counter-rotating propellers: one for displacement running, located in the upper main foil anhedral; and the other for foilborne running, located at the lower main foil intersections. The single propeller of Rx affects yaw and turning circle performance, and its inclined thrust line produces a different thrust-drag moment. This increases bow foil loading with speed from the nominal static value of 10% of the all-up weight to 16% at 25 knots.

The all-up weight of Rx increased from 6640 lb, during early trials, to 7300 lb, during 1965 trials, mainly because of foil changes and added spray protection for crew and equipment. The estimated all-up weight of FHE-400 also increased during the period and was given as 474,000 lb in July 1965, making Rx about 3½% underweight in 1965 trials.

Maximum speed of Rx is 28.5 knots in calm water, which dynamically corresponds to 57 knots full scale. One important effect of the comparatively low quarter-scale speeds is that cavitation conditions are not correctly represented, and Rx results are valid only if FHE-400 succeeds in operating free of cavitation.

### Trials Instrumentation

The craft is equipped with extensive instrumentation to measure motional, propulsive, and force data. These have usually been recorded by a galvanometer oscillograph, but magnetic tape recording was used for certain sea trials when data were to be presented in the form of power spectral densities. The instrumentation is located mainly in the watertight compartment shown in Fig. 4 and is operated remotely by a trials observer in the front cockpit. A separate 28-v d.c. gasoline-electric generator provides a constant supply voltage independent of the main power plant.

Flight-test components are used extensively, including a vertical gyroscope with potentiometer pick-offs for pitch and roll measurements and rate gyroscopes for pitch, roll, and yaw rate. Unbonded strain-gage transducers are used for pitch and roll angular accelerations and also for most linear acceleration measurements. More sophisticated servo accelerometers are used for sea trials when magnetic tape recording makes it desirable to combine high accuracy and resolution with high-signal output voltage.

Table 1 Original Rx foil system data

Foil panel	Incidence	Chord, in.	Section
Bow anhedral	1° 40'	16.0	7½% NACA 16-40
Upper bow dihedral	1° 40'	12.0	7½% NACA 16-40
Lower bow dihedral	1° 24'	8.0 to 16.0	7% Walchner C
Main anhedral	1° 40'	30.0	7½% NACA 16-40
Main dihedral	1° 24' to 3° 54'	18.0 to 30.0	7% Walchner C
Main horizontal	1° 24'	18.0	7% Walchner C
Main anhedral tip extension	1° 40'	30.0 to 15.0	7½% NACA 16-40

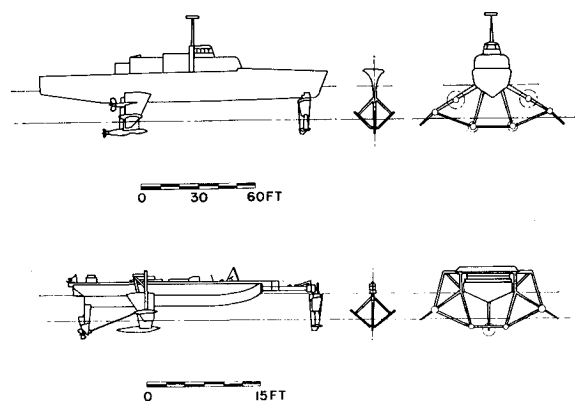


Fig. 5 Outline comparison with FHE-400.

The propeller shaft and bearing assemblies were designed to incorporate bonded strain-gage transducers for shaft torque and thrust measurements, and Fig. 7 shows these arrangements in detail. The propeller shaft and thrust bearing assemblies are arranged to be slip-free in the direction of the shaft axis, and end restraint is provided entirely by a strain-gaged yoke at which the thrust measurement is made. The propeller shaft is driven from the V-gearbox by an outer concentric shaft, and this is equipped with strain gages and slip rings to provide shaft torque measurements.

Bonded strain-gage lift, drag, and sideforce measuring elements were designed and built into the main foil structure by DeHavilland and are shown in part in Fig. 8. The lift balance elements are four slender, vertical pillars which connect the foil beam structure to the hull. This is strengthened locally and made more rigid by a tubular-steel stabilizing framework fitted athwartships at the beam mountings. The vertical pillars are strain-gaged and interwired so that electrical outputs caused by axial strain are added for all four pillars, whereas those caused by bending strains and temperature effects are canceled. Because the four lift pillars are relatively long and slender, they introduce little side constraint. This is provided by port and starboard strain-gaged ring dynamometer drag links and a single sideforce measuring link. Measurements made at the bow foil include steering loads, helm angle, and the midspan strains at the dihedral panels. The strain gages and wiring are accommodated in slots, ½ in. deep in the foil upper surfaces, filled flush with epoxy resin to preserve the surface contours. A similar technique is used to measure the midspan strain of the horizontal panel of the main foil.

Forward speed was determined on many straight calm water runs by timing over a measured course approximately ¼ mile in length. These runs were also used to calibrate a pitot-static head located with the two associated strain-gage pressure transducers at the starboard main foil intersection pod.

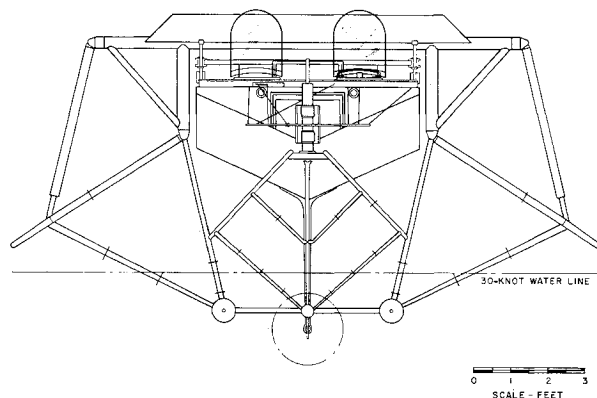


Fig. 6 Early foil elevation.

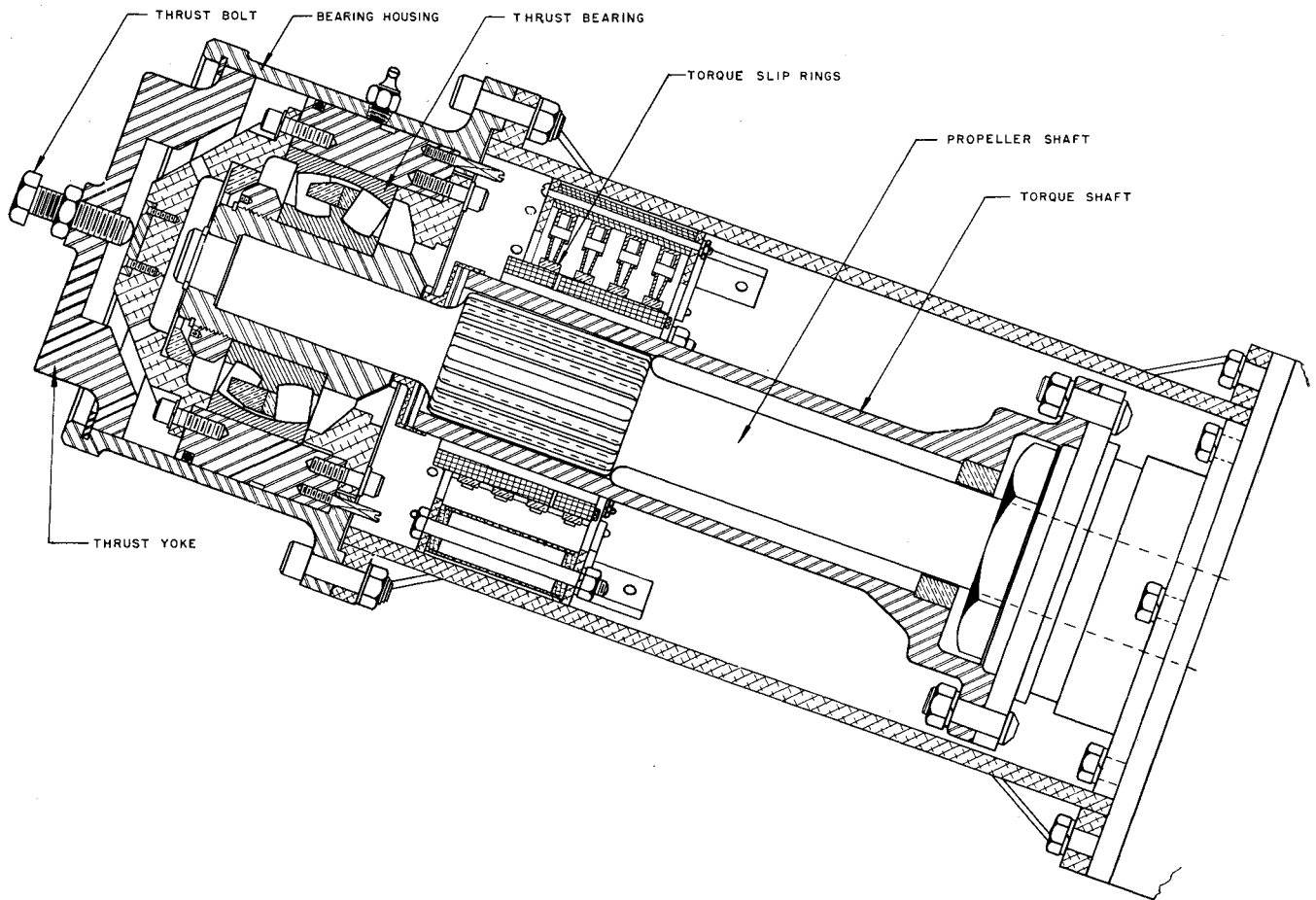


Fig. 7 Torque and thrust measurement.

### Results: Early Bow Foil Development

It was recognized from the outset that the design of a bow foil for operation at 50 knots in a seaway would present many difficulties. Fluctuations of immersion and angle of attack due to wave action and ship pitch would be more pronounced at the bow than at the main foil and could well lead to serious cavitation and ventilation. At the same time, the performance of the lightly loaded bow foil would have a profound effect on system performance as a whole because it acts as a "feeler" to provide inherent trim stabilization.

The original bow foil designed by DeHavilland was fitted with conventional delayed-cavitation sections, and ventilation immediately became a problem, even in calm water. Anti-ventilation fences were used liberally, as shown in Fig. 9, and

effected good control until a fence broke surface when ventilation spread abruptly to the next lower fence. This was satisfactory at low foilborne speeds because considerable foil area was immersed, and the percentage loss of lift remained small. At higher speeds, however, with comparatively little foil area immersed, a large percentage of the total available lift was lost and pitch stability was affected. At 23 knots, for example, with the waterline at the midspan fences of the lower dihedral foils, almost complete immersion of the bow foil unit with very slow recovery resulted from ventilation jumping to the lower fences.

Anticipating the superiority of supercavitating sections for this design, DeHavilland had provided alternative lower dihedral foils as shown in Fig. 10a. Supercavitating sections are essentially sharp-nosed, well-cambered, and set at high angles of incidence. Lift is generated almost entirely by the lower surface, and the only restriction on the upper surface is that it must be thin enough to lie completely within the cavity which originates from the leading edge. The lift-drag ratio of a supercavitating section is comparatively low but is acceptable for the FHE-400 bow foil because it carries only 10% of the weight. The particular section used for Rx had a Tulin-Burkart two-term lower surface<sup>3</sup> and was set at 7° incidence, as shown in Fig. 10a.

Continuous ventilation proved hard to achieve, particularly during initial transition from wetted to ventilated flow and in rough water. At low speeds, with flow fully attached, the high incidence and camber developed very high lift and caused trim to increase rapidly with speed to a value of 4° at 8 knots. (High trim at low speed remained a characteristic of the system throughout the development, as shown by Fig. 11, the trim-speed curves for a late stage in the trials.) The original foils ventilated at about 14 knots, and the sudden decrease in lift allowed the bow foil to plunge deeply into the

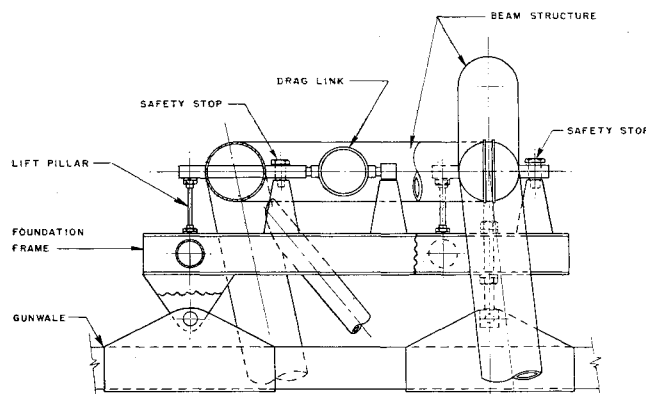


Fig. 8 Main foil lift and sideforce dynamometers.

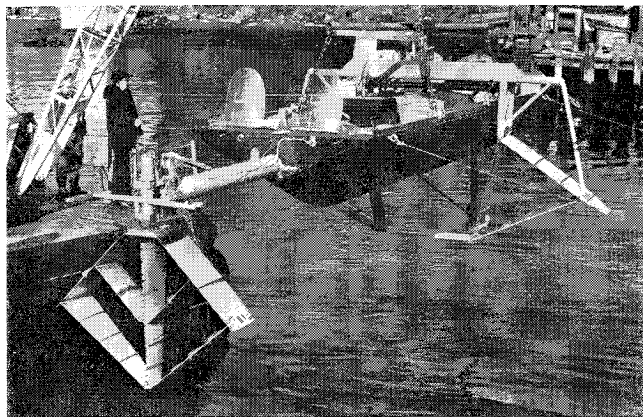


Fig. 9 Early FHE-400 foils.

water. Flow promptly reattached, and high lift was restored to cause a severe cyclic pitching motion. It was necessary to increase bow foil rake from  $0^\circ$  to  $+3^\circ$ , thus setting the incidence of the supercavitating foils to a nominal  $+10^\circ$  in order to achieve stable running over even a limited speed range.

Stable running at  $0^\circ$  rake setting was later achieved at all speeds above 19 knots by fitting leading-edge spoilers to the upper surfaces of the supercavitating foils, as shown dotted in Fig. 10a. Rough-water tests at this time were limited to 20 to 25 knot runs through 2 to  $2\frac{1}{2}$ -ft high waves in tug wakes, but performance in this vital aspect was very encouraging and resulted in continued development of the bow foil using supercavitating sections.

Leading-edge spoilers are undesirable because they increase both spray and drag. They were removed and the section was modified, as shown in Fig. 10b, by making it finer over the first third of its chord, thereby improving the range of angles of attack over which the section lay entirely within the cavity. The modified section ventilated stably on Rx at speeds above 15 knots and rake settings as low as  $-1^\circ$  although cyclic pitching persisted in the transition speed range between  $12\frac{1}{2}$  and 16 knots. Unfortunately, foilborne runs through waves of only moderate slope now produced pronounced pitching motions; and it was clear that, although tolerance to angle of attack had been improved, the section remained too subject to flow reattachment for satisfactory use in a seaway.

DeHavilland again modified the section, this time by the addition of a spoiler at the 60% chord point, as shown dotted in Fig. 10b. In this location, the spoiler prohibited large lift increases by preventing flow reattachment over the heavily cambered after-section but, being well within the ventilation envelope at high speeds, contributed little extra drag or spray.

The performance in a seaway was greatly improved by this modification, and successful trials were made at 25 knots in waves which ranged in severity up to short breaking seas 5 to 6 ft in height. The liveliest motions were in head and bow seas when the bow foil frequently left the water, although the crew felt no shock on re-entry. Under the worst conditions, the main foil also tended to leave the water and this was followed by a noticeable squatting and deceleration; but, despite the comparatively low hull clearance, no hull pounding occurred.

The performance of the system in severe following and quartering seas is of particular interest since foil operating conditions are then particularly adverse, and, in fact, most surface-piercing systems have failed in following seas. Accelerations seemed less severe to the crew than in head and bow seas although recorded amplitudes were similar, and only frequencies were reduced. The craft was run for distances of between 1 and 2 miles at speeds up to 25 knots in the worst sea conditions with no sign of diving or broaching-to. There was a greater tendency to roll and steering control was reduced, but lateral stability and directional control were always adequate.

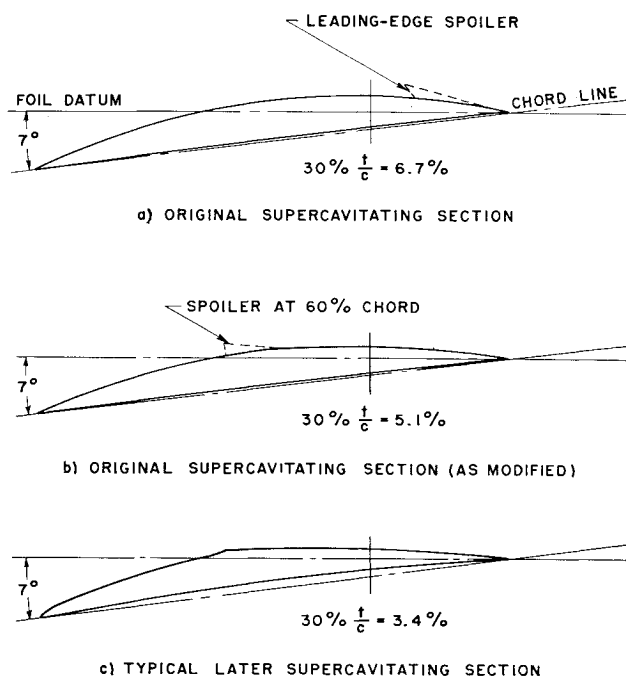


Fig. 10 Supercavitating sections.

### Results: Final Bow Foil Development

Sea trials experience with the original superventilating bow foil was good, but modification of the design was desirable to reduce the drag and improve the pitch response in a head sea. DeHavilland redesigned the unit completely, deleting the upper dihedral panels and developing the required lift characteristics from the single diamond configuration shown in Fig. 12. Supercavitating sections are now used throughout, with Tulin-Burkart two-term lower surfaces retained but with about double the camber of the previous sections. The spoiler at 60% chord, essential to the success of the previous section, is now built into the upper surface contour. The form of the new section is shown in Fig. 10c.

Production of this unit marked the end of major bow foil development changes. Rx continued to perform well in calm and rough water but unfortunately, before tests could be completed, the new bow foil unit was torn from its mounting and lost in collision with a derelict timber structure floating submerged in the harbor. A replacement unit was built which

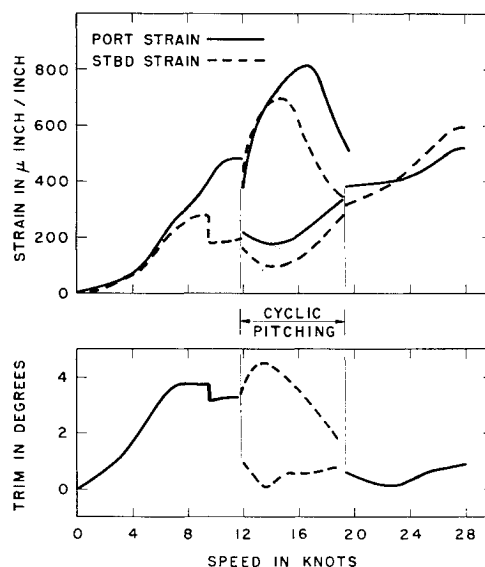


Fig. 11 Strain and trim—speed characteristics.

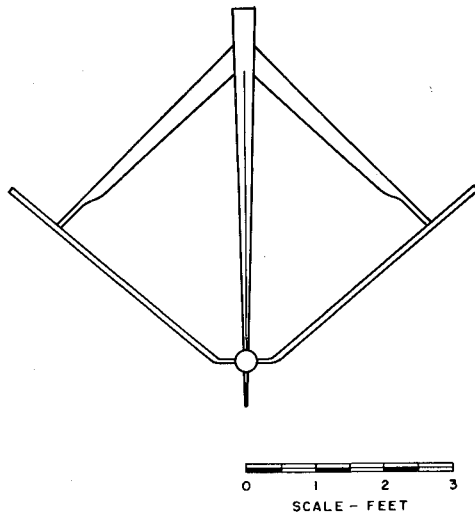


Fig. 12 Final bow foil elevation.

incorporated some minor refinements in planform and section, but both calm- and rough-water trials results for the two units proved very similar.

Typical calm-water behavior is illustrated in Fig. 11. This shows the trim changes for a run at slowly increasing speed at  $0^\circ$  foil rake setting in conjunction with bow foil strain, which proved a useful indicator of ventilation and flow reattachment on the foil panels. The sharp step down in starboard panel bending strain at  $9\frac{1}{2}$  knots was due to ventilation from the leading edge, and there was an associated trim decrease of over  $\frac{1}{2}^\circ$ . Ventilation of the port panel just below 12 knots led to a further trim decrease and initiated the by then familiar cyclic pitching instability, and this persisted to  $19\frac{1}{2}$  knots. Subsequently, a further section modification and refinement of the outboard intersections was made to insure a steady flow of air to the dihedral foils, and this has virtually eliminated the cyclic pitching.

The effect of the fully developed bow foil on system performance in a seaway is the most important consideration, but sea trials data are difficult to analyze and compare because of the random character of the waves and lack of control over conditions for a particular trial. There are restrictions on the method, but, in practice, the usual way is to reduce the data to the form of power spectral densities and use these to define the statistical properties of the waves and the various craft motional and structural characteristics. The power spectral density function for the seaway  $G_x(f)$  is related to that for a particular craft characteristic, e.g., pitch-angle amplitude

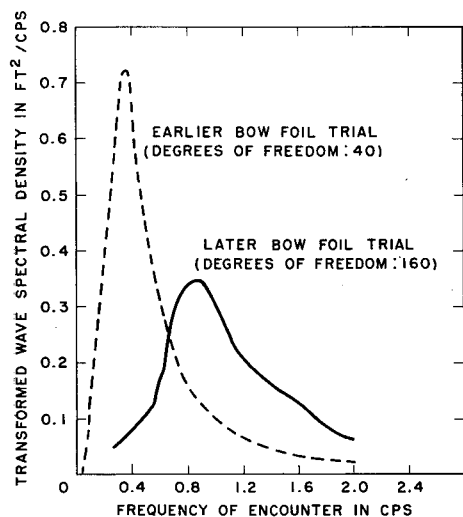


Fig. 13 Sea state power spectral densities.

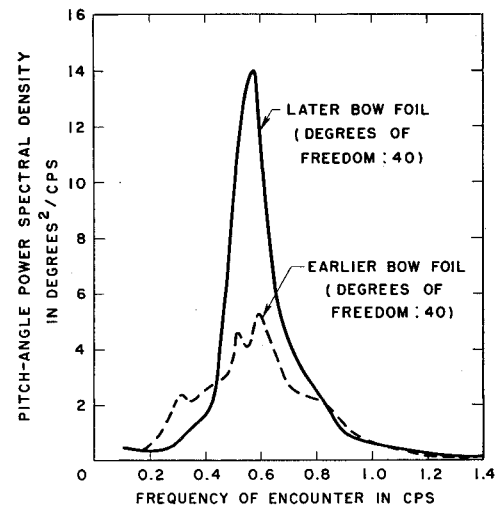


Fig. 14 Pitch amplitude power spectral densities.

$G_y(f)$  by the expression,  $G_y(f) = H(f)^2 G_x(f)$ , Ref. 4, where  $H(f)$  is the frequency response function, in this case, for pitch angle. The hydrofoil system is not linear over wide amplitude excursions, but use of this expression nevertheless enables comparison of basic changes in system characteristics despite the different sea states in which trials must inevitably be made.

Wave amplitude spectra are shown in Fig. 13 for sea trials with the early (part superventilating) bow foil and the later refined version. The original data were obtained using an anchored wave pole and were recorded on magnetic tape as amplitude-time histories. For use with the foregoing expression, they must be transformed to the frequencies of encounter appropriate to the Rx trial speed and direction to the seas (in this case, 25 knots in a head sea). The rms values derived from the power spectra are given in Table 2, together with estimates for the means of the  $\frac{1}{3}$ -highest waves, based on a Rayleigh distribution of peak values since the spectra are comparatively narrow. The corresponding power spectral density functions for pitch angle and vertical acceleration at the c.g. are given in Fig. 14 and 15 and the rms and amplitude estimates in Table 2.

Both the period and amplitude of pitching increased with the later bow unit, as shown by the comparative frequency response functions of Fig. 16; and these changes resulted in a softer ride and a reduced tendency for the bow and main foils to leave the water, although the bow foil became completely immersed more often in steep seas. The better riding characteristics at 25 knots in a head sea are demonstrated very

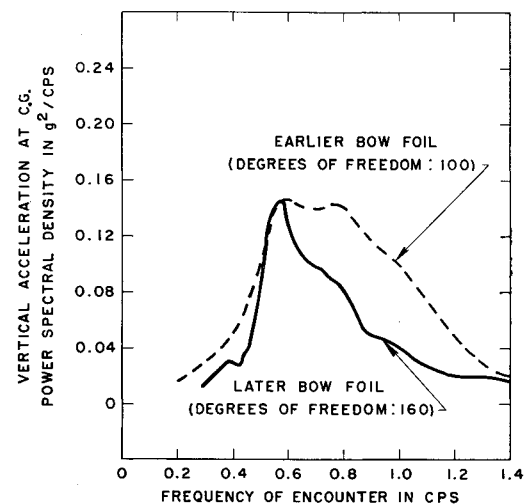


Fig. 15 Vertical acceleration power spectral densities.

Table 2 Sea trials data

	Earlier bow foil		Later bow foil	
	rms value	Mean top third	rms value	Mean top third
Sea state	0.62 ft	2.5 ft	0.64 ft	2.6 ft
Pitch	1.5°	6.0°	1.8°	7.3°
Vertical acceleration at c.g.	0.34 g	1.4 g	0.25 g	1.0 g

clearly in Fig. 17. This compares the response functions for vertical acceleration at the c.g. (the single most important criterion of rough-water performance) and shows it to have been greatly reduced both in level of response and in the peak frequency.

### Results: Main Foil Development

Main foil development was not pursued as actively with Rx as was bow foil development partly because the behavior of the subcavitating sections was better understood and amenable to conventional small-scale model work and partly because the required changes were comparatively difficult to make. Development changes were necessary, however, to improve roll stability.

As speed increased from rest, the craft began to heel until at 13 knots there was a 5° loll which switched, apparently arbitrarily, from port to starboard. At about 15 knots, this developed into cyclic rolling with a typical amplitude of 8° and a period of 5½ sec. Rolling ceased at 19 knots and the craft became very stable; but at 23 knots, when the original short anhedral tips (Table 1) left the water, the craft heeled sharply and sideslipped off the foils.

DeHavilland modified the main foil configuration by extending the anhedral tips to the 30-knot waterline, increasing the tip-incidence angles from 1°40' to 3°20', and changing the section to 5% Engineering Research Associates No. 1.<sup>2</sup> High-speed roll stability was excellent with this arrangement both in calm and rough water, but the problem remained at low speed.

No serious attempt was made to improve low-speed roll stability until the redesigned bow foil unit was first fitted, at which time the chord and camber of the anhedral main foil panels were increased substantially at the inboard end, giving the tapered planform seen in Fig. 5. This modification succeeded in reducing the steady angle of loll for speeds up to about 11 knots, but cyclic rolling continued between 11 and 19 knots.

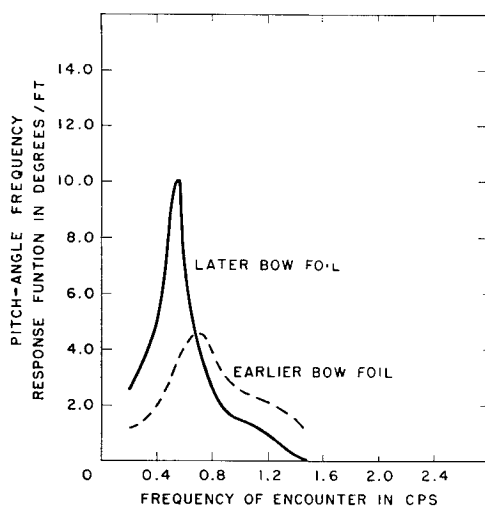


Fig. 16 Pitch amplitude frequency response.

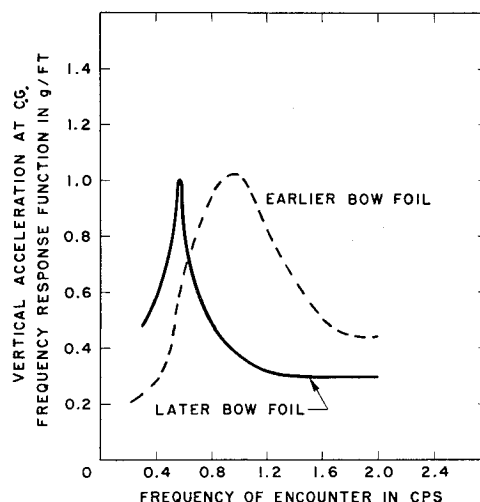


Fig. 17 Vertical-acceleration frequency response.

DeHavilland stability studies showed insufficient roll stability for the full-scale design at low foilborne speeds, and it was decided to make the full-scale extended anhedral tips incidence-controlled. This complicated and expensive modification was not incorporated in Rx, but the problem continued to be of interest because Rx roll stability was lower than predicted by DeHavilland.

Fairing pods added to the comparatively inefficient outboard intersections brought little improvement, and the trouble was eventually found to be closely associated with the cyclic pitching instability described previously. Trim-angle changes due to cyclic pitching caused heaving at the main foil surfaces and this, aggravated by ventilation of the main anhedral, produced strong cyclic rolling. Interestingly, sharp increases in bow foil strain due to ventilation shutoff were shown by the oscillograph records to be occurring on alternate dihedral elements as roll amplitudes approached maximum (Fig. 18). Thus there was very strong mutual roll-pitch coupling, and cyclic pitching occurred consistently at twice the frequency of cyclic rolling.

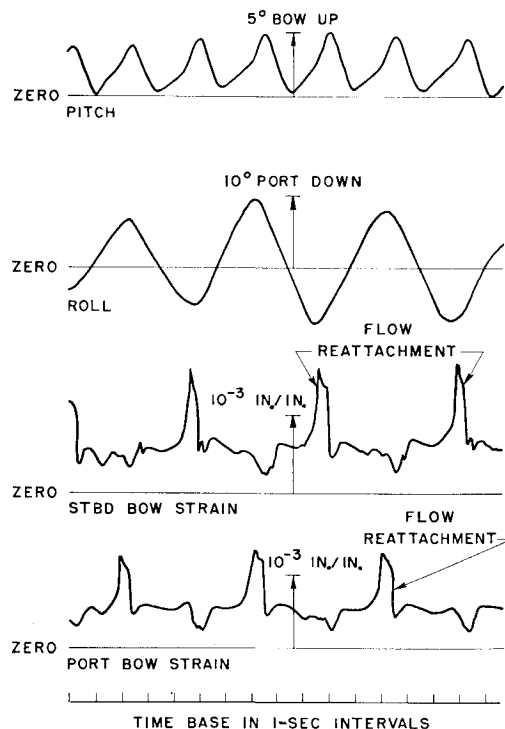


Fig. 18 Coupled pitch-roll oscillation.



This behavior presents an interesting example of the value of Rx tests in demonstrating system characteristics unlikely to have been revealed by theoretical studies, although the elimination of cyclic pitching has now led to the virtual disappearance of cyclic rolling.

### Conclusion

The Rx craft was designed originally to undertake parametric studies on a wide variety of hydrofoil systems, but her greatest use has been in exhaustive testing of the particular system developed for HMCS "Bras d'Or" and, particularly, in the development of a superventilating bow foil unit. The soundness of the original Rx design was demonstrated by her ready adaptability as a quarter-scale version of this ship, and she gave yeoman service by demonstrating in a practical way the capabilities of the system in rough water. She not only verified important design techniques and data but gave positive evidence of certain unexpected deficiencies and assisted greatly in their rectifica-

tion. This experience has emphasized the value of a large-scale manned model with six degrees of freedom in the development of advanced ocean vehicles, and such open-water trials are considered an essential and integral part of the design process.

### References

- <sup>1</sup> Lewis, C. B., "A hydrofoil ship for the Royal Canadian Navy," *SNAME Hydrofoil Symposium, Seattle, Wash., May 13-14, 1965* (Society of Naval Architects and Marine Engineers, New York, 1965), Paper 2-1.
- <sup>2</sup> Richardson, J. R., "The design of hydrofoil profiles," *Final Report, Design Study 180 Ton ASW Hydrofoil Ship, Volume IV, Technical Reports* (The DeHavilland Aircraft of Canada Ltd., Downsview, Ontario, December 1962).
- <sup>3</sup> Tulin, M. P. and Burkart, M. P., "Linearized theory for flows about lifting foils at zero cavitation number," David Taylor Model Basin Rept. C-638. (February 1955).
- <sup>4</sup> Bendat, J. S., *Principles and Applications of Random Noise Theory* (John Wiley & Sons Inc., New York, 1958).

JULY 1967

J. HYDRONAUTICS

VOL. 1, NO. 1

## Internal Thermal Structures in the Ocean

EUGENE C. LAFOND\* AND KATHERINE G. LAFOND  
U. S. Navy Electronics Laboratory, San Diego, Calif.

Advanced equipment makes possible the acquisition of a continuous two-dimensional thermal structure of the upper 240 m of the sea. Shallow-water temperature data were recorded at the Navy Electronics Laboratory Oceanographic Research Tower from horizontally and vertically mounted arrays of thermistor beads. Deep-water temperature data were recorded by a 900-ft towed thermistor chain mounted on the USS Marysville. Detail of these structures reveals many oceanographic processes such as internal waves, turbulence, oceanographic fronts, upwelling, and other types of water motion. The internal structure of both shallow and deep water is made up of a broad spectrum of waves. One dominant oscillation is close to the Väisälä frequency. Common wavelengths fall between 500-800 m in deep water but shorten as they refract across the continental shelf. The wavelengths and direction of propagation are influenced by density and topographic boundaries. Near shore, the changes in depth and strength of the thermal structure are largely controlled by wind transport, in accordance with the Ekman effect. Some internal structures can be ascertained from sea surface slicks and recordings made with airborne infrared equipment.

### Introduction

THE ocean is a composite of many relatively thin layers, each exhibiting different properties. The lightest layer is uppermost, and the more dense layers lie progressively deeper in the sea. These layers are neither flat nor still; they slope in ever-changing patterns of depth, thickness, and angle. Most layers tilt less than one-half deg, but this small shift is a significant clue to many of the internal processes of the sea. Even these small angles which change with time and space can alter the direction of sound rays passing through the boundary layers and influence the bearing and range accuracy of acoustic detection. Changes in internal temperature structures therefore become of primary interest.

The most informative feature of the ocean for acoustic studies is density; but since this is not easily determined, temperature is commonly used because it is one of the easiest

properties to measure and normally controls density. Isothermal oscillations resulting from heat exchange and various water motions have therefore been studied intensively.

The U. S. Navy Electronics Laboratory (NEL), which has been investigating thermal structures in both shallow and deep water, employs separate techniques and equipment for each. For shallow-water studies, both horizontal and vertical fixed arrays are suspended into the sea from the NEL Oceanographic Research Tower. The vertical array of thermistors shows changes in the depth of isotherms, and the circular-horizontal array gives both spacial and time changes. For deep-water studies, a towed 900-ft chain is used to delineate thermal structure.

### Theory

The sea temperature and its resulting thermal structure derive from the heating and cooling of the ocean by sun and sky. The heat is distributed by advective, conductive, and mixing processes through internal and external forces such as wind or tide.<sup>1</sup> Internal waves, which travel at different frequencies, depths, and directions, are also a dispersing factor.

Presented as Preprint 66-692 at the AIAA/USN 2nd Marine Systems & ASW Conference, Los Angeles-Long Beach, Calif., August 8-10, 1966; submitted August 1, 1966; revision received November 28, 1966. [11.02]

\* Head, Marine Environment Division.